Toward Microwave Electromagnetic Jets for Detection, Imaging and Local Characterization Applications

Bruno Sauviac, Ali Ghaddar, Antoine Deubaibe, Bernard Bayard

Toward Electromagnetic Jets for Detection, Imaging and Local Characterization Applications.

B. Sauviac*[a], A. Ghaddar[a], A. Deubaibe[b], H. Hyani[a] and B. Bayard[a]
[a] Université de Lyon, Université Jean Monnet-Saint-Etienne, CNRS, Institut d'Optique Graduate School, [b]Université de Ndjaména, Tchad

ABSTRACT

We present an overview of our latest investigation regarding microwave electromagnetic jet (EMJ) dedicated to detection, imaging and characterization applications. First EMJ proposed is a parallel plate waveguide loaded with Teflon and terminated with both single and dual elliptically shaped tips. The experimental result shows the generation, respectively, of a single or a double EMJ as numerically expected. To simplify the manufacture of the tips, a rectangular tip replaced the elliptical termination. The numerical results demonstrated an increase in intensity and low FWHM of the beam, especially when using a multi-rectangular section of the tip. Furthermore, a rectangular waveguide with a rectangular tip was also introduced as an alternative to produce the EMJ in two transverse directions. Finally, to obtain a rotationally symmetrical jet, a horn antenna loaded with Teflon and ended with a cylindrical Teflon shape was proposed. In term of application, the developed microwave electromagnetic jet demonstrates the capability to detect extremely small objects not detectable by conventional microwave systems. In addition, at the focal point, the jet exhibits an almost planar wavefront, indicating the possibility of using the jet for local characterization applications in mesoscale free space measurements.

Keywords: Photonic jet, electromagnetic jet, FWHM, detection, imaging, focal point, local characterization, free space measurement.

1. INTRODUCTION

Photonic jet (PJ) was originally considered in optics when a laser beam interacted with dielectric nanoparticles [1]. Under specific physical and geometrical conditions of the nanoparticles and the surrounding media, the light beam exhibits intriguing properties, including a high intensity and an extremely short Full Width at Half Maximum (FWHM). The main benefit of the photonic jet lies in the ability to enhance the FWHM by tuning the geometrical dimensions and shapes of the dielectric particles [2]. These characteristics pave the way for various applications based on imaging and detection with high accuracy.

The phenomenon of the PJ was extended also toward low frequencies such us terahertz [3], [4], [5], [6] and microwave [7], [8], [9] referred to as electromagnetic jet (EMJ). The first experimental confirmation of the microwave EMJ was conducted with a cylindrical dielectric object excited by a plane wave in a free-space environment [7]. Subsequently, the phenomenon was applied in a waveguide configuration, integrating a dielectric tip positioned at the terminus of the waveguide for enhanced practical utility [5]. Several studies were done especially in the realm of terahertz technology [5], focused on employing waveguides for imaging and detection purposes. At lower frequencies, in the microwave range, the use of electromagnetic jets is very limited, if not non-existent.

In this letter, we show an overview of our recent work demonstrating these phenomena at microwave frequencies by implementing several microwave systems, including antennas and waveguides equipped with dielectric tips of various geometries. The primary goals of the developed EMJ microwave revolve around applications such as detection, imaging, and local characterization of materials.

2. MICROWAVE ELECTROMAGNETIC JETS

2.1 Parallel plate waveguide

In this section, we present a microwave electromagnetic jet (EMJ) produced using a parallel plate waveguide configuration [10]. Figure 1(a) shows a schematic of the parallel plate waveguide, with an elliptical shape of a Teflon tip extended towards free space. In order to generate a dual EMJ, a tip with a dual elliptical shape is also considered, as shown in Figure

1(b). To produce experimentally an EMJ, a source antenna was positioned in the far field to excite the parallel plate tipped waveguide with TE polarization. The experimental results of a spatial distribution of the electrical field for both single and dual EMJ at 30GHz is presented in Figure 1(c) and (d), respectively. This electric field map was measured using a WR-28 probe held on a robotic arm. The focused beam of a single jet exhibits a Full Width at Half Maximum (FWHM) of approximately 0.6λ. In contrast, the dual jets are generated nearly symmetrically along the axis of the tips, with a FWHM of 0.5λ. The experimental results demonstrate a strong agreement with expected studies carried out numerically with a boundary integral equation model [11].

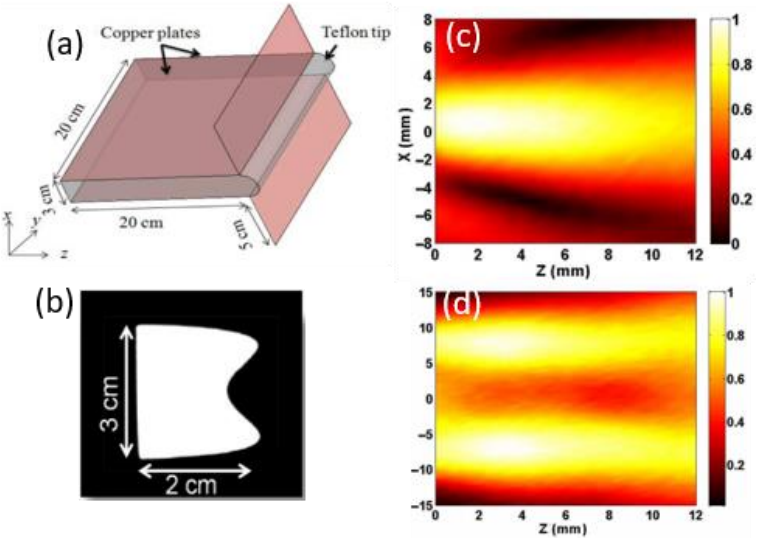

Figure 1. (a) Schematic representation of a parallel plate waveguide with an elliptical Teflon tip. (b) Illustration of the dual elliptical Teflon tip. Electrical field maps resulting from TE polarization of the parallel plate waveguide at 30 GHz, generated with a single (c) and a dual elliptical Teflon tip (d), respectively. [10]

The rectangular shape has replaced the elliptical tip for easier manufacturing. Figure 2 represent an optimized electrical field calculated numerically using aperiodic polynomial modal method [12]. The optimization study involved a multi-rectangular section shape of the tip, comprising one, two, and three sections at 30 GHz. In the case of TE polarization, the results indicate that the FWHM for one, two, and three rectangular sections are 0.42λ, 0.38λ, and 0.36λ, respectively. It is observed that increasing the number of rectangular sections can reduce the FWHM of the jet. This finding was validated also through simulation using commercial HFSS software.

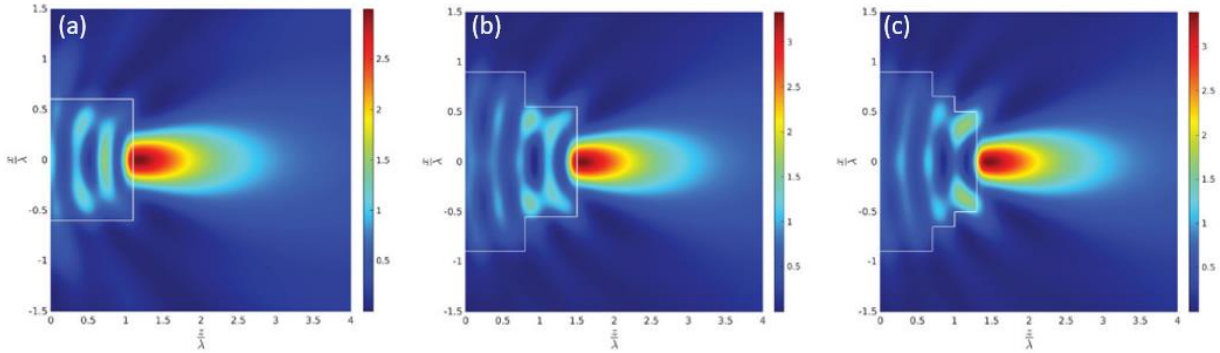

Figure 2. Electric field maps in TE polarization for optimized (a) one section tip (b) two sections tip and (c) three sections tip at 30 GHz. [12]

2.2 Rectangular waveguide

As presented above, the EMJ generated by the parallel plate waveguide exhibit a focused beam with a low FWHM solely in one direction. Hence, a WR-90 rectangular waveguide is proposed with the aim of generating the EMJ in two different directions at 15 GHz. A WR-90 rectangular waveguide loaded with Teflon and terminated toward free space with a rectangular Teflon tip is shown in Figure 3(a). The Teflon tip presents a square cross-section in the xy-plane ($L_x = L_y$). Optimization of the tip dimensions was performed in simulation using Ansys HFSS software with the aim of obtaining a low FWHM value. Additionally, a pyramidal transition region is considered inside the waveguide to improve the impedance matching between the empty and Teflon-loaded waveguide.

The simulated results of the electric field distribution in both directions show a the jet formation with a focal point around 13 mm from the tip's end. Regarding FWHM, it is noted that in the x-direction and y-direction, its values are approximately 0.54λ and 0.39λ, respectively. The difference in FWHM between two directions can be attributed to the distribution of the field within the waveguide. Specifically, inside the rectangular waveguide, the waveform's shape differs between the x-direction and the y-direction because of non-symmetrical section of the waveguide, yielding a non-symmetrical jet even using a square cross-section.

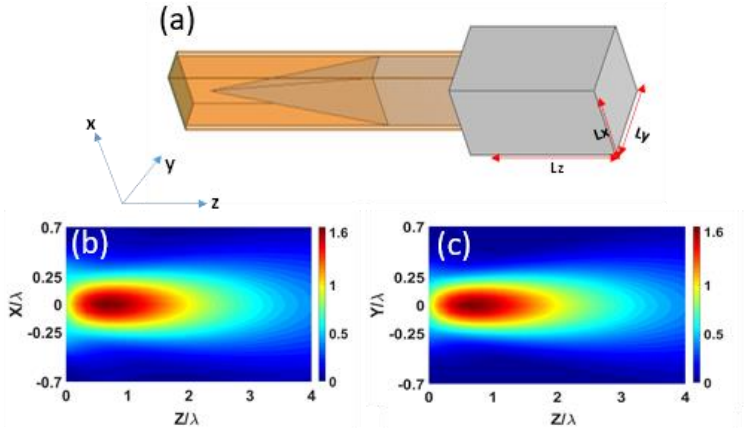

Figure 3. (a) Representation of the electromagnetic jet based on the rectangular waveguide equipped with a loaded Teflon tip of rectangular shape, with its dimensions: $L_x = L_y = 30mm$ and $L_z = 60mm$. (b) And (c) electrical field maps simulated at 15GHz for both xz- and yz-plane.

2.3 Circular horn antenna

We observed that using a cross-section of the tip at the end of rectangular waveguide could generate a jet in both directions, but with different FWHM. In the context of the rectangular waveguide, a symmetric section of the tip is unable to produce a symmetrical jet due to the asymmetrical distribution of the wave inside the waveguide. Here, we show that a circular horn antenna can allow generating a symmetrical spot of the jet by considering a symmetrical section of the tip. In Figure *4*(a), we present a Teflon-loaded horn antenna extended by a cylinder tip. At the antenna input, the Teflon fill is designed to include a transient section that helps improve impedance matching and thus reduce reflection. The cylindrical Teflon tip incorporated at the end of the antenna has a radius of 1 cm and a thickness of 2.2 cm. These geometric parameters were optimized in simulation to achieve high intensity and low FWHM of the beam at 30 GHz. The electric field map measured in yz- and xz-plane are illustrated in Figure 4(b) and (c), respectively. We observe on the maps that the jet is characterized by a high intensity focus located at 5 mm after the end of the tip. The jet generated by this system exhibits an approximate FWHM value of 0.6λ. The advantage of this configuration is to generate a symmetrical distribution of the jet as shown in Figure 4(c).

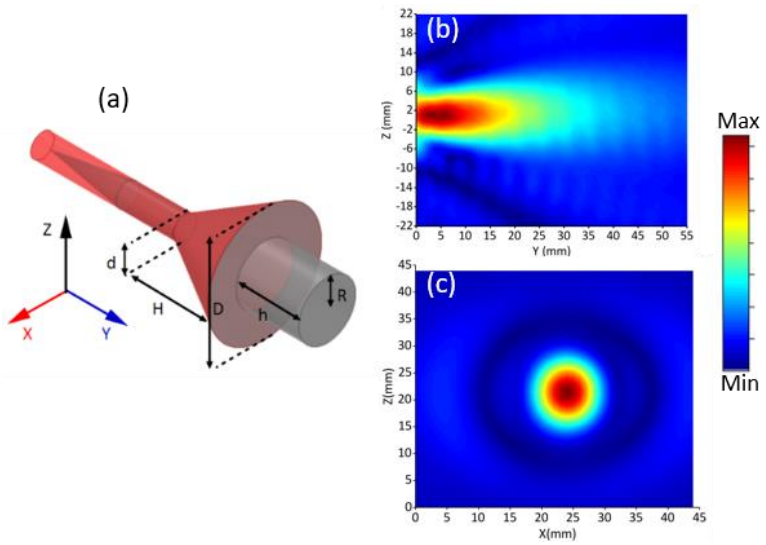

Figure 4. (a) Representation of the horn antenna with dimensions d=0.82cm, H=2.8cm and D=4cm loaded with Teflon extended in free space by a cylindrical tip with dimensions h=2.2cm and R=1cm. Electrical field maps measured at 30GHz in xz-plane (b) and yz-planes at focal point.

3. APPLICATIONS

3.1 Imaging and detection

In this section, we introduce a study conducted to assess the performance of the microwave EMJ for detection and imaging applications. In this context, we illustrate in Figure 5 an example of use for detecting by scanning, rods hidden in an opaque object using the suggested EMJ created with a horn antenna (see the section 2.3). As shown in Figure 5(b), mapping the amplitude of the measured reflection reveals a significant response associated with the presence of the different rods inserted in the opaque object. The maps make it possible to successively distinguish the four rods which are not all at the same depth from the surface. The two rods positioned in the center, having similar maximum responses, correspond to the metal rods of dimension λ/50. The PVC rod, located at the very bottom of the card, is also visible and identifiable. As for the metal rod having the largest diameter λ/10, is transversely located at the very top, the low amplitude detected is explained by its deeper position compared to the rods placed in the middle. This study shows us the performance of EMJ in detecting rods and distinguishing them according to their immersion inside the material.

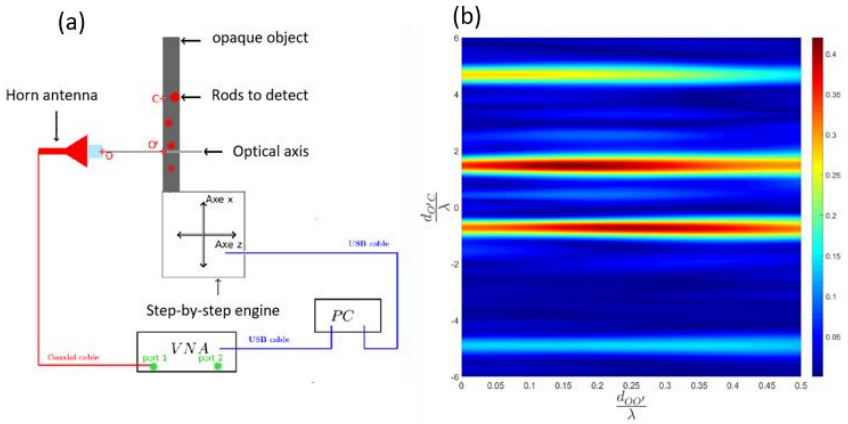

Figure 5. (a) Representation of the experimental bench used to detect the metallic and dielectric rods hidden inside an opaque material. (b) Mapping of the amplitude of the reflection coefficient detected using the experimental bench illustrated by the schema presented on the left. [13]

3.2 Local characterization

In addition to detection and imaging, the EMJ can be a promising means for the local characterization of materials while remaining in a very short distance from the material under test. To understand why EMJ can be utilized for local characterization applications, the simulated mapping field is plotted both inside the Teflon tip and within a material situated behind the jet as presented in Figure 6(a). As observed, jet formation occurs due to the propagation velocity disparity between the free space and the Teflon tip. In addition, the wavefront exhibits a local planar behavior within the substrate. This characteristic of the wave enables the measure reflection coefficient close to that calculated by Maxwell's equation under classical plane wave condition; this opens the way to local material characterization applications.

To explore this hypothesis, we measured the response using the jet and compared to the theoretical response of the material illuminated by a plane wave; this approach therefore enables us to experimentally evaluate this local characterization capability. Measurements of the reflection coefficient were conducted using an FR4 Epoxy substrate with a permittivity of $\varepsilon_r = 4.4(1 - j\,0.04)$ and a thickness of 1.6 mm. The substrate comprises bare sections separated by metallized areas, with the widths of these sections decreasing gradually as illustrated in the experimental set-up (width 3, 2 and 1cm) which can be seen in Figure 6(b)). The evolution of the module and the phase of the reflection coefficient measured by scanning along the sample at the frequency 30 GHz is presented in Figure 6(c) and (d), also shown the theoretical values of the module and the phase calculated at 30 GHz for the FR4 substrate and the metal part. It is noted that the module of the measured reflection coefficient corresponds to the same theoretical values of -5 dB and 0 dB when the jet traverses, respectively, the non-metallized and metallized parts including the smallest part with a width of 1 cm. It can also be noted that the measured phase presents values close to the theoretical values of the non-metallized and metallized substrate, which are respectively 2.7 and 3.14 radians. In the FR4 substrate section, a maximum difference of about 0.12 radians compared to theory is observed. This variation remains acceptable and can be attributed to the short-circuit calibration condition that was applied to the metallized part, which has a slight thickness difference around 70µm compared to the bare surface.

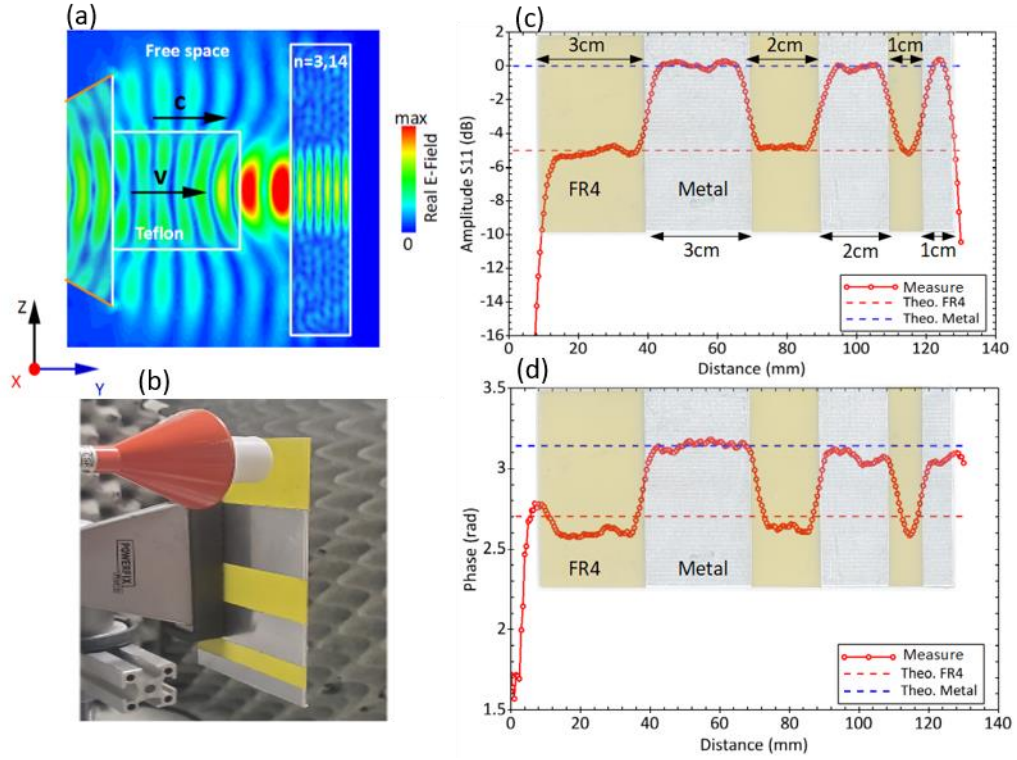

Figure 6. (a) Map of the E field (real part) representing the evolution of the wave through the tip and inside the material placed 5 mm from the end of the tip. (b) Experimental bench for characterization of an FR4 Epoxy sample consisting of bare and metallized parts of width 3, 2 and 1 cm. Module (a) and phase (b) of the reflection coefficient S_{11}. The curve with red circle represents the experimental result (Measure). The dotted line curves represent the theoretical values at 30 GHz (Theo.) for FR4 Epoxy and metal.

4. CONCLUSION

This letter presented an overview of our recent advancements in microwave EMJ technology operating in 15 and 30 GHz. Various microwave systems have been proposed for generating an EMJ, including parallel plate or rectangular waveguides, as well as circular horn antennas. The interaction of diffractive waves exiting from microwave devices toward free space has been studied using various tip shapes, such as elliptical, rectangular, and cylindrical. It is shown that the dual elliptical tip could produce a dual jet. In addition, a rectangular section and multi-section were proposed respectively to simplify the manufacturing and to enhance the FWHM of the focused beam. The outcomes indicate that both the waveguiding system and the tip's shape notably affect the formation of the jet. It was demonstrated that the parallel plate could generate the jet in only one direction. Conversely, we observed that the rectangular waveguide facilitated jet generation in two directions but without rotational symmetry, whereas the circular horn antenna exhibited this rotational symmetry at the focal point.

In terms of application, our studies illustrate the microwave jet's ability to detect and image metallic and dielectric rods with very low diameters compared with the wavelength, concealed within opaque materials. Finally, we also demonstrated the potential of employing the concept of the jet to locally characterize materials in the mesoscale.

5. REFERENCES

[1] Z. Chen, A. Taflove, et V. Backman, « Photonic nanojet enhancement of backscattering of light by nanoparticles: a potential novel visible-light ultramicroscopy technique », *Opt. Express*, vol. 12, nº 7, p. 1214, 2004, doi: 10.1364/OPEX.12.001214.

[2] I. Minin et O. Minin, *Diffractive optics and nanophotonics: resolution below the diffraction limit*. in SpringerBriefs in physics. Cham Heidelberg New York Dordrecht London: Springer, 2016. doi: 10.1007/978-3-319-24253-4.

[3] V. Pacheco-Peña, M. Beruete, I. V. Minin, et O. V. Minin, « Terajets produced by 3D dielectric cuboids ».

[4] H. H. N. Pham, S. Hisatake, O. V. Minin, T. Nagatsuma, et I. V. Minin, « Enhancement of spatial resolution of terahertz imaging systems based on terajet generation by dielectric cube », *APL Photonics*, 2024.

[5] S. Hisatake et E. Miyake, « Terahertz scanning microscopy with 2λ depth of field based on photonic nanojet generated by a dielectric cuboid probe », *Opt. Express*, vol. 30, nº 25, p. 45303-45311, déc. 2022, doi: 10.1364/OE.472209.

[6] J. Calvo-Gallego, « Enhancing resolution of terahertz imaging systems below the diffraction limit », *Optics and Laser Technology*, 2023.

[7] A. Heifetz, K. Huang, A. V. Sahakian, X. Li, A. Taflove, et V. Backman, « Experimental confirmation of backscattering enhancement induced by a photonic jet », *Appl. Phys. Lett.*.

[8] S.-C. Kong, A. V. Sahakian, A. Heifetz, A. Taflove, et V. Backman, « Robust detection of deeply subwavelength pits in simulated optical data-storage disks using photonic jets », *Appl. Phys. Lett.*.

[9] L. Zhao et C. K. Ong, « Direct Observation of Photonic Jets and Corresponding Backscattering Enhancement ».

[10] B. Ounnas, B. Sauviac, Y. Takakura, S. Lecler, B. Bayard, et S. Robert, « Single and Dual Photonic Jets and Corresponding Backscattering Enhancement With Tipped Waveguides: Direct Observation at Microwave Frequencies », *IEEE Trans. Antennas Propagat.*, vol. 63, nº 12, p. 5612-5618, déc. 2015, doi: 10.1109/TAP.2015.2491328.

[11] Y. Takakura, S. Lecler, B. Ounnas, S. Robert, et B. Sauviac, « Boundary Impedance Operator to Study Tipped Parallel Plate Waveguides », *IEEE Trans. Antennas Propagat.*, vol. 62, nº 11, p. 5599-5609, nov. 2014, doi: 10.1109/TAP.2014.2347391.

[12] S. R. Hishem Hyani Bruno Sauviac, Gérard Granet, Bernard Bayard et K. Edee, « Electromagnetic jet produced with loaded waveguide ended by an optimized multi-rectangular sections tip », *Journal of Electromagnetic Waves and Applications*, vol. 37, nº 18, p. 1587-1596, 2023, doi: 10.1080/09205071.2023.2262984.

[13] H. Hyani, « Jet électromagnétique 3D : détection, imagerie et contrôle non destructif dans des structures opaques. », p. 141, PhD Thesis, Doctoral school of Saint-Etienne, 2021.